Piyasena, R.K.N.P., Farha, M.F.F., Hewage, I.S., Young, S.M. and Halwatura, R.U., 2026. Iron slag substitution in soil-based geopolymers: A comparative study with coal fly ash for non-load bearing applications. In: Waidyasekara, K.G.A.S., Jayasena, H.S., Chandanie, H. and Tennakoon, G.A. (eds). *Proceedings of the 14th World Construction Symposium*, 10-11 July 2026, Sri Lanka. pp. 1022-1036. DOI: https://doi.org/10.31705/WCS.2026.75. Available from: https://ciobwcs.com/papers/

IRON SLAG SUBSTITUTION IN SOIL-BASED GEOPOLYMERS: A COMPARATIVE STUDY WITH COAL FLY ASH FOR NON-LOAD BEARING APPLICATIONS

R.K.N.P. Piyasena[1], M.F.F. Farha[2], I.S. Hewage[3], S.M. Young[4] and R.U. Halwatura[5]

ABSTRACT

The production of traditional Ordinary Portland Cement (OPC) drives significant greenhouse gas emissions, necessitating a shift toward sustainable, low-carbon building materials. This study investigates the development of geopolymerized mud concrete (GMC) by valorizing two industrial by-products—coal fly ash (CFA) and iron slag (IS)—as primary aluminosilicate precursors. The research aimed to establish baseline parameters for a reference CFA-based GMC, optimize an IS-substituted alternative, and evaluate its comparative feasibility. Microstructural characterization confirmed both materials possess essential glass-forming oxides. While CFA relies on abundant silica and alumina to develop robust aluminosilicate networks, IS drives binder formation through complex Fe-A-S-H and C-A-S-H gels. Utilizing an alkaline activator comprising 10M sodium hydroxide and 2% sodium chloride, the methodology was included in two phases. First, optimal thermal curing conditions were established for the 20% CFA reference. Subsequently, to maximize mechanical performance, IS substitution levels (10% to 40%), curing temperatures (ambient to 100 °C), and durations (6 to 24 hours) were systematically optimized through 7-, 14-, and 28-day compressive strength testing. The benchmark CFA mix (cured at 100 °C for 6 hours) achieved a peak 28-day compressive strength of 3.241 MPa. Conversely, the optimized IS matrix (30% IS, cured at 60 °C for 24 hours) attained 1.601 MPa. Although yielding approximately 49% of the CFA baseline capacity, the 1.601 MPa IS-based geopolymer satisfies requirements for non-load-bearing masonry. Ultimately, this study demonstrates that IS is a resilient, low-cost, and eco-friendly precursor alternative that advances circular economy principles, particularly in regions lacking accessible CFA reserves.

Keywords: *Alkaline Activation; Coal Fly Ash; Compressive Strength; Geopolymerized Mud Concrete; Iron Slag Valorisation.*

---

[1] Research Assistant, Department of Civil Engineering, University of Moratuwa, Sri Lanka, nethmi97praba@gmail.com
[2] Student, Department of Environmental Technology, University of Colombo, Sri Lanka, farhafareed2000@gmail.com
[3] Research Assistant, Department of Civil Engineering, University of Moratuwa, Sri Lanka, iresharesearch1@gmail.com
[4] Professor, Department of Environmental Technology, University of Colombo, Sri Lanka, sansfica@et.cmb.ac.lk
[5] Senior Professor, Department of Civil Engineering, University of Moratuwa, Sri Lanka, rangikauh@gmail.com

1. INTRODUCTION

The construction industry is under increasing pressure to reduce its environmental footprint due to intensive energy consumption, heavy reliance on non-renewable raw materials, and substantial greenhouse gas emissions. Ordinary Portland Cement (OPC), the primary binder in conventional concrete, is responsible for approximately 5–7% of global anthropogenic CO_2 emissions (Singh & Middendorf, 2020; Mohan et al., 2025). At the same time, the construction sector consumes nearly 40% of global energy resources and contributes to severe land degradation through extensive quarrying of limestone and other minerals (United Nations Environment Programme, 2023). In response to these challenges, geopolymer concrete (GPC) has emerged as a promising, eco-friendly alternative. By utilizing aluminosilicate-rich industrial by-products activated with alkaline solutions, GPC can reduce embodied carbon by up to about 80% compared with OPC-based systems, while achieving comparable mechanical performance (Juenger et al., 2011; Mohan et al., 2025).

Parallel to the development of low-carbon binders, there is renewed interest in sustainable earth-based construction. Mud concrete, a soil-based composite typically comprising soil, cement, and water, is valued for its low cost, local availability, and thermal comfort. However, its dependence on OPC limits its environmental benefits (Arooz, 2019; Arooz & Halwatura, 2018). To overcome this, the concept of geopolymerized mud concrete (GMC) has been introduced by Udawattha & Halwatura (2018), in which the cementitious fraction is replaced by alkali-activated industrial by-products rich in alumina (Al_2O_3) and silica (SiO_2). GMC integrates the climate-responsive advantages of mud construction with geopolymer technology, enabling significant reductions in clinker use while aligning with circular economy principles through waste valorisation.

Among potential GMC precursors, coal fly ash (CFA) and iron slag (IS) are particularly attractive but form chemically distinct binder systems. CFA-based geopolymers are typically low-calcium, forming N–A–S–H–type aluminosilicate gels and often requiring elevated curing temperatures (60–80°C) to accelerate dissolution and strength gain, especially at high fly-ash contents (Zhao et al., 2021; Wijepala et al., 2022). These systems offer excellent thermal and chemical stability at high temperatures, but strength development and workability are highly sensitive to activator concentration, silicate/NaOH ratio, and curing regime (Shi et al., 2021; Chen et al., 2024). In contrast, Fe-rich alkali-activated, where C-(N)-A-S-H and Fe-A-S-H gels dominate and can achieve high early strength and dense microstructures under more moderate curing conditions (often ambient to 70 °C) (Zhang et al., 2021). While increased slag content generally enhances early compressive strength and interfacial bonding, it may reduce high-temperature residual strength compared with fly-ash-dominant systems, revealing a strength–durability trade-off between CFA and IS based binders (Zhang et al., 2021).

These mechanistic differences have practical implications for low-cost masonry. CFA-based systems tend to be more reliant on controlled, often higher-temperature curing to reach target strength, whereas Fe-rich systems can attain comparable or higher mechanical performance at lower curing temperatures but may be more sensitive to fracture behavior, pore structure, and high-temperature degradation (Zhang et al., 2021). Critically comparing CFA and IS based activation pathways is therefore essential to select curing regimes and precursor blends that are both energy-efficient and mechanically robust for non-load-bearing earth masonry (Nath & Kumar, 2013).

In Sri Lanka, substantial deposits of ancient iron-smelting slag exist in regions such as Yodhawewa, while CFA is widely generated by local thermal power plants. The utilization of these specific industrial residues in construction directly supports the transition toward a circular economy and contributes to the United Nations Sustainable Development Goals, particularly SDG 12 (Responsible Consumption and Production) and SDG 13 (Climate Action). By reducing demand for virgin raw materials, diverting waste from landfills, and lowering the carbon intensity of masonry units, geo-polymerized mud concrete can play a pivotal role in sustainable development.

Accordingly, this study aims to: (i) establish the optimal thermal curing conditions for a reference CFA-based GMC; (ii) determine the optimum precursor substitution level, curing temperature, and curing duration required to maximize the compressive strength of an IS-based GMC; and (iii) evaluate the comparative feasibility of the resulting IS-based material as a resilient, low-cost building solution for non-load-bearing applications. Ultimately, this research contributes to the development of low-carbon masonry products tailored for regions with abundant industrial by-products, minimizing reliance on OPC and non-renewable earth resources.

2. MATERIALS AND METHODS

A previously developed systematic approach for GMC, as outlined by Udawattha and Halwatura (2018) and Gayashani et al. (2025), was followed to prepare and test the proposed IS and CFA-based GMC. The procedures were based on relevant standard guidelines for material characterization, mix design, specimen preparation, and performance evaluation.

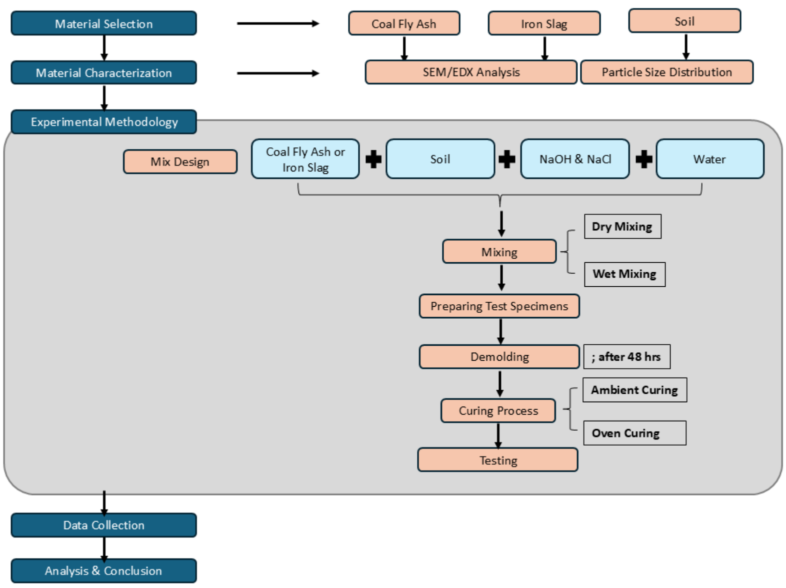

Figure 1: Developed experimental framework of the study

2.1 MATERIAL SELECTION, COLLECTION, AND PREPARATION

The materials used to produce the novel GMC comprised locally available soil, aluminosilicate precursors iron slag (IS) and coal fly ash (CFA) and an alkaline activator system of sodium hydroxide (NaOH) and sodium chloride (NaCl). Soil was excavated from a homogeneous layer approximately 600 mm below ground level at the University of Moratuwa premises to minimize organic matter and surface disturbances. Following the removal of visible organic debris, the soil was dried to eliminate free moisture. Sieve analysis (BS 1377-2:1990) was then conducted to verify gradation consistency with prior GMC studies.

IS was sourced from Palugaswewa, Anuradhapura, where it exists abundantly as an underutilized byproduct of iron-smelting activities, while CFA was obtained from the Lakvijaya Coal Power Plant. Both IS and CFA samples were characterized using SEM-EDX to examine their morphology, phase texture, and elemental composition, confirming their suitability as geopolymer precursors. Following characterization, the IS was ground to a fine powder, and particles passing a 75 µm sieve were selected to enhance dissolution and reaction kinetics during alkali activation (Lee et al., 2021). Similarly, the CFA was sieved through a 150 µm sieve to remove coarse particles and improve homogeneity (Haustein & Kuryłowicz-Cudowska, 2020).

The alkaline activator system consisted of analytically pure NaOH and NaCl. Commercial NaOH pellets with a purity of 99 wt% were dissolved in water to prepare the main activating solution, providing hydroxide ions necessary to dissolve silica (SiO_2) and alumina (Al_2O_3) from the aluminosilicate precursors and soil matrix. NaCl was incorporated as a secondary additive to increase the ionic strength of the pore solution and to introduce chloride ions, which can influence dissolution, early-age reaction rates, and setting behavior in alkali-activated systems.

2.2 CHARACTERIZATION OF MATERIALS

2.2.1 Characterization of Soil Type

The natural soil serving as the primary matrix in the GMC was characterized through a detailed particle size distribution analysis to assess its engineering suitability. Sieve analysis was conducted in accordance with BS 1377-2:1990, following standard geotechnical practices for grading granular soils. The results confirmed that the soil is a heterogeneous mixture of gravel, sand, and fines, typical of construction soils used in stabilized earth and soil–cement systems (Wang et al., 2025).

Based on the analysis, the soil comprises 39.62% gravel (> 4.75 mm sieve), 55.22% sand (0.075 mm – 4/75 mm), and 5.16% fines (< 0.075 mm sieve). Gradation parameters derived from the particle size distribution curve (Figure 2) show an effective grain size D_{10} of 0.428 mm, alongside D_{30} and D_{60} values of 1.918 mm and 4.704 mm, respectively. From these values, the coefficient of uniformity ($C_u = D_{60}/D_{10}$) was calculated as 10.99, and the coefficient of curvature ($C_c = D_{30}^2/(D_{10}\times D_{60})$) as 1.83, following conventional soil mechanics definitions used to describe particle size distribution.

According to the Unified Soil Classification System (USCS), $C_u > 6$, $1 < C_c < 3$ and a 5–12% fines content, the soil is classified as a well-graded sand with silt (SW–SM). The obtained grading and classification align with soils previously employed in geo-polymerized or stabilized earth systems, where controlled gradation optimizes packing density and mechanical performance (Ferreira et al., 2023; Wang et al., 2025).

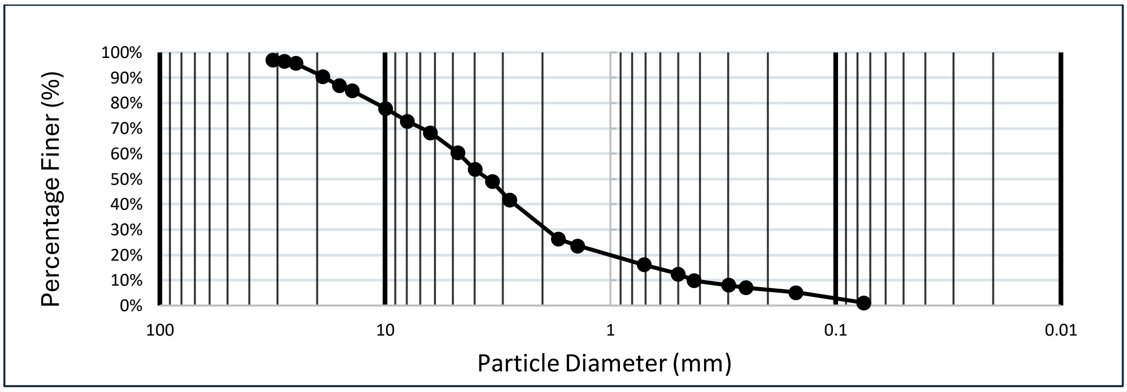

Figure 2: Particle size distribution curve for soil

This well-graded nature is highly advantageous for GMC, as a continuous particle size distribution minimizes the void ratio and enhances packing to improve overall strength and durability. Ultimately, the selected gradation provides a robust granular skeleton, facilitating the development of a dense, mechanically efficient geopolymerized matrix (Ferreira et al., 2023).

2.2.2 Characterization of Iron Slag

The microstructural and chemical characteristics of the iron slag (IS) were evaluated using SEM-EDX spectroscopy to assess its viability as a reactive geopolymer precursor, following standard methodologies for Fe-rich alkali-activated systems (Nikolov, 2020).

SEM imaging across 1.00K× to 15.00K× magnifications (Figure 2) revealed a heterogeneous assemblage of subrounded to subangular particles. At higher magnifications, the slag exhibits rough, porous, and irregular surface textures. This angularity is highly advantageous for mechanical interlocking within the concrete matrix. Furthermore, the intrinsic porosity significantly increases the specific surface area available for alkaline dissolution, facilitating the development of a dense geopolymeric network (Wang et al., 2024).

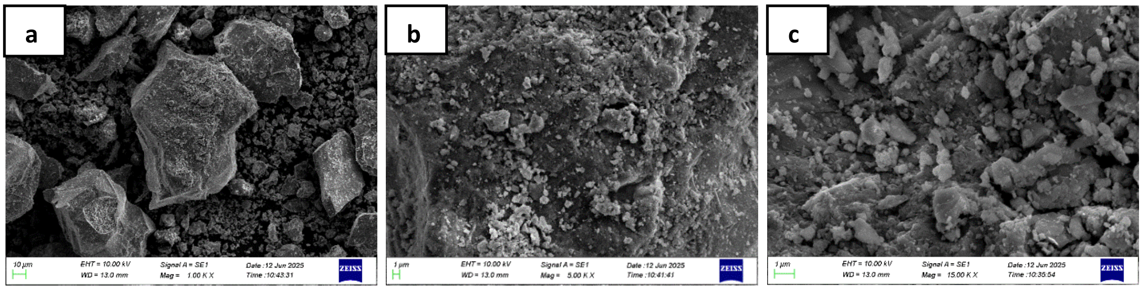

Figure 3: Surface morphology of iron slag - (a) 10 µm size, 1.00 K × magnification, (b) 1µm size, 5.00 K × magnification, (c) 1 µm size, 15.00 K× magnification

The elemental composition of the slag was quantified by EDX, with the spectrum and quantitative results presented in Table 1 and Figure 4. The slag is identified as a high-iron precursor, containing approximately 41.18 wt% Fe, accompanied by reactive oxides such as Si (8.76 wt%), Ca (2.56 wt%), and Al (4.21 wt%), along with minor Mg, Mn, and K. Typical Fe-rich metallurgical slags used in alkali-activated materials exhibit comparable Fe–Si–Ca–Al chemistries, often described within a $CaO–FeO_x–SiO_2–Al_2O_3$ system (Nikolov, 2020).

Table 1: Elemental composition of iron slag

Element	**Fe**	**Al**	**Si**	**Ca**	**C**	**O**	**Mg**	**P**	**K**	**Ti**	**Mn**
wt%	41.18	4.21	8.76	2.56	8.60	29.28	0.86	0.00	0.39	0.20	3.96
Atom%	18.73	3.96	7.92	1.62	18.19	46.48	0.90	0.00	0.25	0.10	1.83

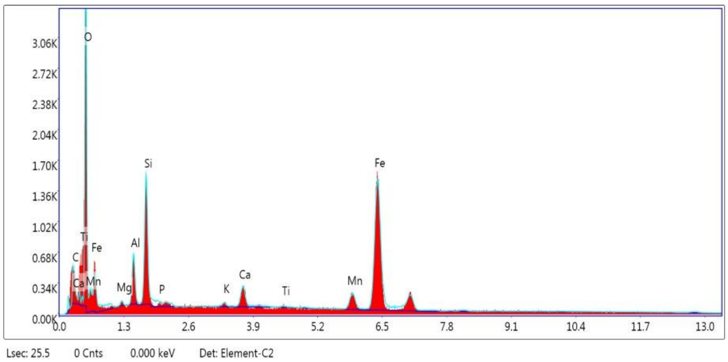

Figure 4: Elemental composition spectrum of iron slag

The high Fe content of the slag, together with appreciable amounts of silica and alumina, promotes the formation of complex Fe–A–S–H and C–A–S–H gels (often alongside C–(N)–A–S–H in mixed systems) under alkali activation, which act as the main binding phases responsible for strength gain and microstructural densification in Fe-rich and slag-rich alkali-activated materials (Lee & Lee, 2015; Wang et al., 2024). These reaction products enhance early-age strength, reduce pore connectivity, and improve durability, including resistance to chemical attack and elevated temperatures in Fe-rich systems.

2.2.3 Characterization of Coal Fly Ash

The microstructural and chemical properties of the CFA were characterized via SEM-EDX spectroscopy to evaluate its viability as an aluminosilicate precursor for geopolymerization.

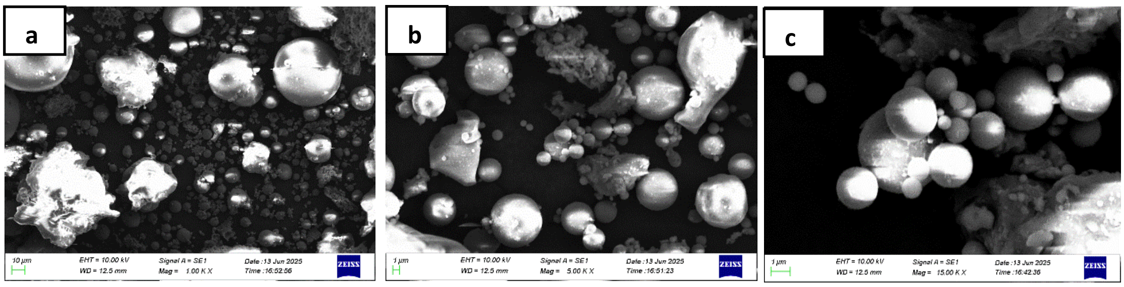

Figure 5: Surface morphology of coal fly ash - (a) 10 µm size, 1.00 K × magnification, (b) 1µm size, 5.00 K × magnification, (c) 1 µm size, 15.00 K× magnification

SEM observations at magnifications from 1.00K× to 15.00K× (Figure 4) show that the CFA is a heterogeneous material comprising spherical, irregular, and fine-detritic particles, consistent with the typical morphology of bituminous coal fly ash morphology (Strzałkowska, 2020). The sample is dominated by smooth-surfaced spherical particles, including a substantial proportion of hollow cenospheres, which are characteristically enriched in silica and alumina. These spherical forms enhance pozzolanic reactivity and improve mix workability via a “ball-bearing” effect, which reduces viscosity and facilitates optimal particle packing, thereby supporting the suitability of the CFA as a precursor for geopolymer binder synthesis (Ma et al., 2021).

EDX analysis (Table 2 and Figure 6), confirms a high concentration of glass-forming oxides essential for geopolymerization. The primary reactive constituents are silica (21.61 wt%) and alumina (12.13 wt%), complemented by notable concentrations of iron (6.48 wt%) and calcium (3.77 wt%). These compositional attributes are consistent with the requirements for Class F fly ash under ASTM C618, a category widely recognized for its efficacy in sustainable geopolymer applications due to its low CaO content and high amorphous phase fraction (Strzałkowska, 2020).

Table 2: Elemental composition of coal fly ash

Element	Si	Al	Ca	Fe	C	O	Na	Mg	K	Ti
wt%	21.61	12.13	3.77	6.48	9.99	43.06	0.17	0.60	1.29	0.90
Atom%	15.28	8.93	1.87	2.30	16.51	53.44	0.15	0.49	0.66	0.37

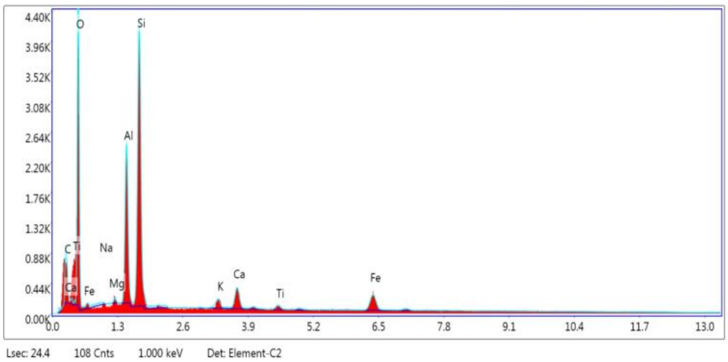

Figure 6: Elemental composition spectrum of coal fly ash

The significant combined concentrations of Silica and Alumina are instrumental in facilitating rapid dissolution under alkaline activation. This chemical process leads to the subsequent formation of complex aluminosilicate gels, which serve as the primary binding phases responsible for strength development and microstructural densification within the geopolymer matrix (Pławecka et al., 2022).

2.3 MIX DESIGN AND OPTIMIZATION PROCEDURE

2.3.1 Initial Reference Mix

Traditional geopolymer concrete mix designs frequently rely on strict stoichiometric molar ratios (such as precise Si/Al or Na/Al elemental targets) or empirical trial-and-error approaches centred purely on workability. However, these conventional alternative methods are often inadequate for soil-based geopolymer systems due to the high physical and chemical heterogeneity inherent in natural soils. Due to the wide variability in precursor materials and the absence of universally accepted guidelines for geopolymer concrete mix design, proportions are typically established through empirical optimization and existing literature.

Accordingly, the initial mix design for this study was adopted from the CFA-based GMC framework proposed by Udawattha and Halwatura (2018). This specific empirical framework was selected over alternative stoichiometric methods because it explicitly accounts for the variable particle size distribution of earth-based matrices. By specifically integrating the fine, sand, and gravel fractions of the soil, this method successfully optimizes the granular skeleton to minimize voids and ensure structural integrity in mud concrete systems. The reference mix was proportioned by total dry weight, comprising 78% soil, 20% CFA as the primary aluminosilicate precursor, and 2% sodium chloride (NaCl) to increase the ionic strength of the pore solution. To ensure an optimal granular skeleton, the soil fraction was graded to include 5% fines (< 0.425 mm), 55% sand (0.425–4.75 mm), and 40% gravel (4.75–20 mm). For alkaline activation, a 10 M sodium hydroxide (NaOH) solution was prepared using pellets of 99% purity. Finally, the water content was maintained at 15–20% of the total dry mass to ensure adequate workability without compromising the material structural integrity.

2.3.2 Optimization Strategy

The optimization of the proposed GMC was conducted in two sequential phases to enhance its overall mechanical performance.

Phase I investigated the influence of curing temperature on the compressive strength of the CFA-based reference mix. To identify the thermal conditions requisite for maximum geopolymeric reactivity and strength development, specimens were subjected to a 6-hour curing period under four specific regimes: ambient temperature, 60°C, 80°C, and 100°C.

Following the thermal optimization of the reference mix, Phase II investigated the functional substitution of CFA with iron slag. The objective was to determine to what extent an iron slag-based GMC could achieve or replicate the maximum compressive strength of the established CFA reference mix. To achieve this, the mix design was systematically refined by evaluating three critical variables concurrently: IS substitution levels (10%, 20%, 30%, and 40% of total dry weight), curing temperatures (ambient, 60 °C, 80 °C, and 100 °C), and curing durations (6, 8, 16, and 24 hours).

2.4 MIXING, CASTING, CURING, AND TESTING PROCEDURE

The experimental programme utilized a systematic procedure to ensure the homogeneity of the GMC and the reliability of the mechanical performance. All concrete mixes were prepared using a mechanical mixer under controlled laboratory conditions, employing a two-stage process to promote uniform constituent dispersion and minimize segregation. In the initial dry-mixing stage, the sieved soil, selected precursor (iron slag or coal fly ash), and NaCl were blended for approximately 10 minutes to establish a consistent, homogeneously distributed solid phase prior to alkaline activation.

During the subsequent wet-mixing stage, the 10 M alkaline solution was gradually incorporated to prevent sudden workability loss and maintain appropriate rheological properties. The total mixing duration was strictly maintained at 20 minutes while visually monitoring consistency. After that, a flow table test (BS EN 12350-5:2009) was conducted to assess workability. The fresh GMC was then cast into 100 mm × 100 mm × 100 mm steel cube molds (BS EN 12390-2:2019) and compacted to eliminate entrapped air, ensuring uniform density. Specimens were retained in the molds for 48 hours under ambient laboratory conditions before demolding to facilitate adequate initial setting and preserve early-age structural integrity.

Following demoulding, specimens were subjected to specific curing temperatures (ambient, 60°C, 80°C, or 100°C) for designated durations (6, 8, 16, or 24 hours), depending on the optimization requirements. Upon completing the thermal cycle, these specimens were transferred to ambient laboratory conditions until testing, allowing further maturation of the geopolymeric binder.

Finally, mechanical performance was evaluated via uniaxial compressive strength testing in accordance with BS EN 12390-3:2002. For each mix proportion, three cube specimens were tested at curing ages of 7, 14, and 28 days. The averaged compressive strength values were used to assess strength evolution and determine the influence of mix composition and thermal curing on the final mechanical behaviour of the GMC.

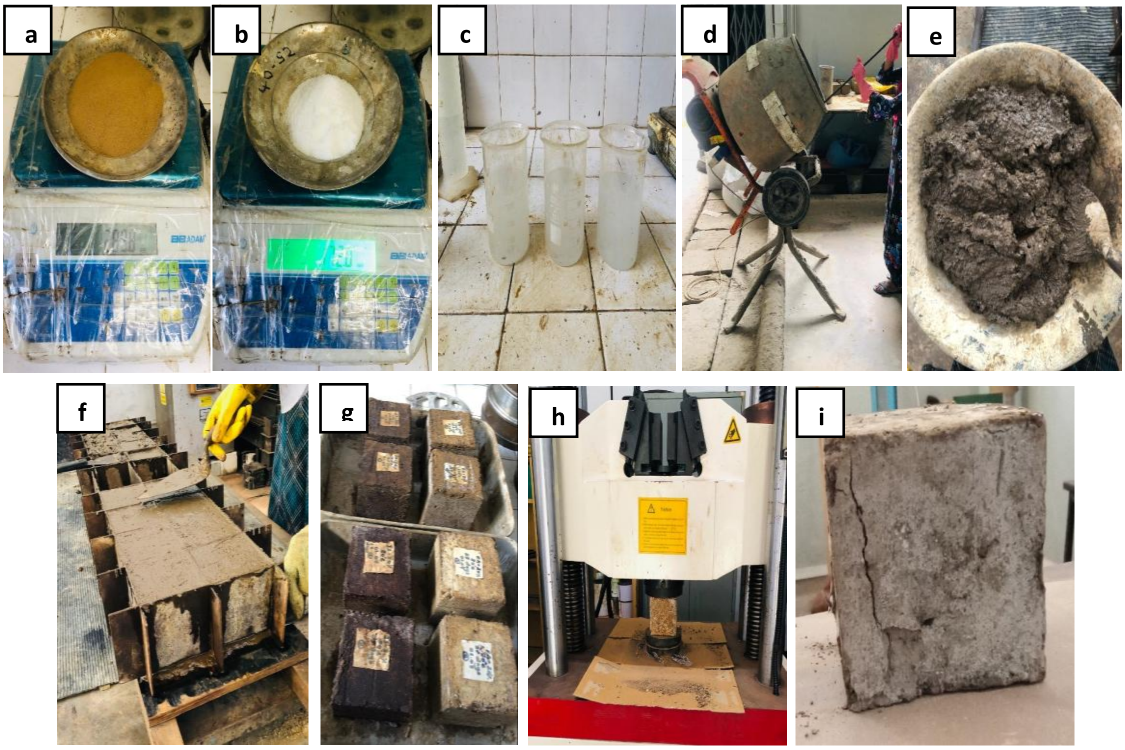

Figure 7: Experimental work (a), (b) measuring materials, (c) preparing NaOH solution, (d), (e) preparing concrete mix, (f) casting test specimens, (g) curing process, (h) testing specimens using UTM, (i) tested specimen

3. RESULTS AND DISCUSSION

To rigorously assess the statistical significance of the experimental variables, all compressive strength data presented in this study were evaluated using a one-way analysis of variance (ANOVA) followed by Tukey's Honestly Significant Difference (HSD) post-hoc test using the MINITAB software.

3.1 PHASE I: OPTIMIZATION OF CURING TEMPERATURE FOR CFA-BASED GMC

As summarized in Table 3, the thermal regime profoundly influences the rate and extent of geo-polymerization, yielding statistically significant differences in both 14-day ($F(3,8) = 7.16$, $p = 0.0118$) and 28-day ($F(3,8) = 31.82$, $p < 0.001$) compressive strengths.

Table 3: Compressive strength (Mean ± SD) under various curing temperatures

Sample Code	14-Day Comp. Strength (MPa)	28-Day Comp. Strength (MPa)
CFA-RT	0.95 ± 0.44[b]	2.37 ± 0.28[b]
CFA-60 °C	0.86 ± 0.35[b]	1.69 ± 0.27[c]
CFA-80 °C	2.75 ± 0.12[a]	3.14 ± 0.20[a]
CFA-100 °C	1.84 ± 0.99[ab]	3.24 ± 0.06[a]

Note: Values within the same column sharing the same superscript letter are not significantly different from each other ($p > 0.05$) based on Tukey's HSD test.

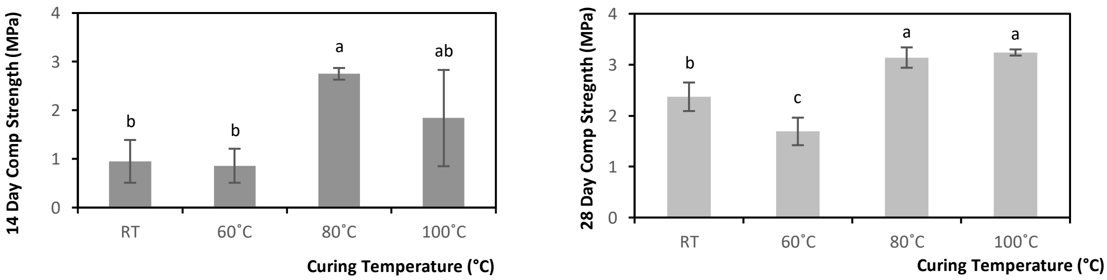

Figure 8: Effect of curing temperature on 14 and 28-Day compressive strength of CFA- based GMC

Although the 100 °C curing regime achieved the highest numerical strength at 28 days (3.24 MPa), the 80 °C regime demonstrated superior early-stage performance (2.75 MPa) and avoided the high statistical variability caused by rapid moisture loss. Consequently, while both elevated temperatures reached statistical equivalence in long-term strength development, 80 °C provides a more stable and reliable thermal environment for optimizing structural growth in coal fly ash-based systems.

3.2 PHASE II: PRECURSOR SUBSTITUTION AND PARAMETER REFINEMENT

3.2.1 Optimization of Iron Slag Content

Following the baseline characterization, Phase II evaluated the substitution of coal fly ash with iron slag at four levels: 10%, 20%, 30%, 40% of the total dry weight. The statistical summary is presented in Table 4.

Table 4: Compressive strength (Mean ± SD) of GMC at varying iron slag contents

Sample Code	7-Day Comp. Strength (MPa)	14-Day Comp. Strength (MPa)	28-Day Comp. Strength (MPa)
IS-10%	0.11 ± 0.03[c]	0.12 ± 0.00[d]	0.21 ± 0.08[c]
IS-20%	0.14 ± 0.02[c]	0.22 ± 0.03[c]	0.31 ± 0.04[bc]
IS-30%	0.54 ± 0.06[a]	0.66 ± 0.02[a]	0.70 ± 0.02[a]
IS-40%	0.26 ± 0.02[b]	0.34 ± 0.07[b]	0.41 ± 0.03[b]

Note: Values within the same column sharing the same superscript letter are not significantly different from each other ($p > 0.05$) based on Tukey's HSD test.

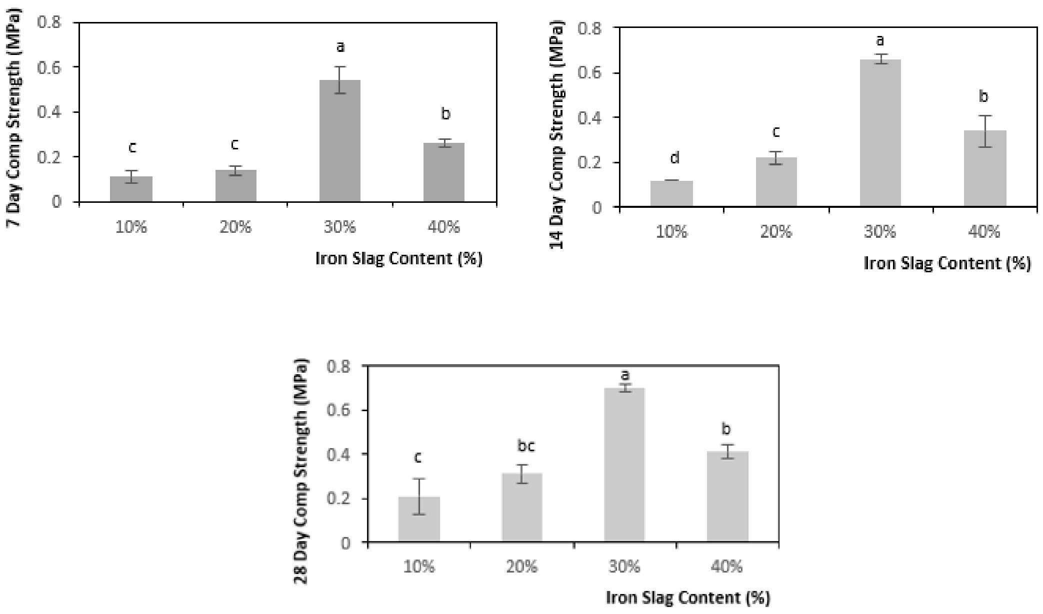

Figure 9: Effect of IS replacement content on the compressive strength of GMC at 7, 14, & 28 Days

As illustrated in Table 3 and Figure 9, compressive strength exhibited a distinct parabolic trend, peaking significantly at 30% substitution. This optimal formulation delivered rapid early-age strength (0.535 MPa at 7 days) and a maximum 28-day capacity of 0.698 MPa. Conversely, increasing the slag content to 40% sharply reduced the 28-day strength to 0.410 MPa. This degradation likely stems from precursor agglomeration and an imbalanced Si/Al ratio, which hinders uniform particle dissolution and disrupts matrix integrity, firmly establishing 30% as the optimal replacement ratio.

3.2.2 Optimization of Curing Temperature

Following the selection of the 30% iron slag formulation, the thermal curing regime was optimized across four environments: ambient, 60°C, 80°C, and 100°C.

As detailed in Table 5 and Figure 10, curing temperature significantly dictates mechanical performance. Compressive strength peaked significantly at 60 °C, yielding 0.76 MPa at 14 days and 1.49 MPa at 28 days, proving statistically superior to all other thermal regimes.

Table 5: Compressive strength (Mean ± SD) of 30% iron slag-based GMC at varying curing temperatures

Sample Code	14-Day Comp. Strength (MPa)	28-Day Comp. Strength (MPa)
IS-RT	0.18 ± 0.02^{d}	0.56 ± 0.09^{b}
IS-60 °C	0.76 ± 0.05^{a}	1.49 ± 0.24^{a}
IS-80 °C	0.43 ± 0.03^{c}	0.61 ± 0.05^{b}
IS-100 °C	0.56 ± 0.07^{b}	0.66 ± 0.08^{b}

Note: Values within the same column sharing the same superscript letter are not significantly different from each other ($p > 0.05$) based on Tukey's HSD test.

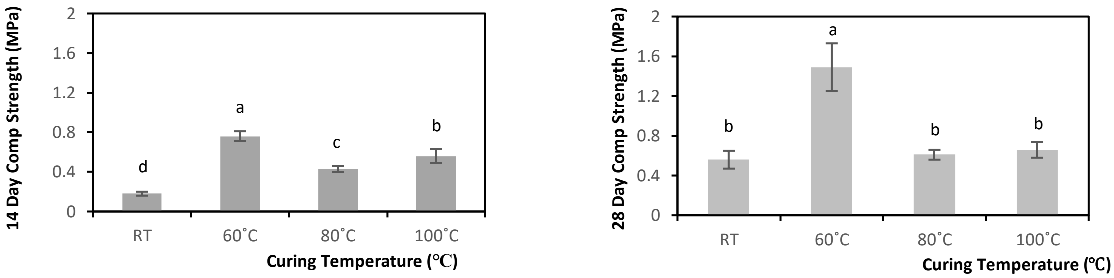

Figure 10: Effect of curing temperature on the compressive strength of 30% iron slag-based GMC at 14 & 28 days

These findings align with existing literature Hao et al., (2025) on slag-based geopolymers which demonstrates that higher temperatures cause strength degradation due to rapid moisture loss and shrinkage cracking. Consequently, 60°C is established as the optimal curing temperature for structural development within this matrix.

3.2.3 Optimization of Curing Duration

Following the determination of optimal precursor substitution (30% iron slag) and temperature (60 °C), the final phase evaluated curing durations of 6, 8, 16, and 24 hours. The statistical summary is presented in Table 6.

Table 6: Compressive strength (Mean ± SD) of optimized IS-based GMC at varying curing durations

Sample Code	7-Day Comp. (MPa)	14-Day Comp. (MPa)	28-Day Comp. (MPa)
IS-6hrs	0.26 ± 0.04^{c}	0.52 ± 0.06^{c}	0.82 ± 0.04^{c}
IS-8hrs	0.32 ± 0.04^{bc}	0.66 ± 0.06^{bc}	1.06 ± 0.11^{bc}
IS-16hrs	0.47 ± 0.08^{ab}	0.75 ± 0.05^{b}	1.25 ± 0.12^{b}
IS-24hrs	0.58 ± 0.08^{a}	0.98 ± 0.06^{a}	1.60 ± 0.11^{a}

Note: Values within the same column sharing the same superscript letter are not significantly different from each other ($p > 0.05$) based on Tukey's HSD test.

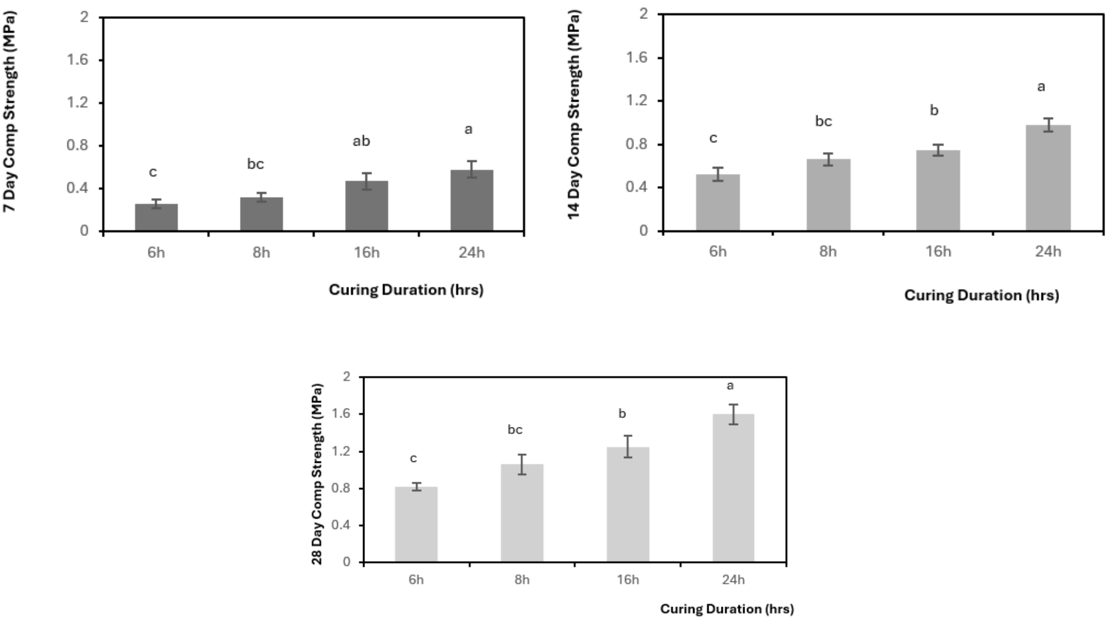

Figure 11: Effect of curing duration on the compressive strength of optimized IS-based GMC at 7,14, & 28 days

As illustrated in Table 6 and Figure 11, extending the curing period to 24 hours produced a progressive, statistically significant increase in compressive strength across all testing ages. This 24-hour regime yielded peak capacities of 0.58 MPa at 7 days, 0.98 MPa at 14 days, and 1.60 MPa at 28 days, significantly outperforming the shorter duration.

These results align with Verma and Nigam (2023), which demonstrating that prolonged thermal exposure drives polycondensation kinetics, facilitating thorough aluminosilicate dissolution and the precipitation of denser gel networks. Furthermore, a 24-hour curing period provides an optimal kinetic window that maximizes structural development without inducing the thermal shrinkage risks associated with over-curing. Consequently, 24 hours at 60 °C is definitively confirmed as the optimal curing regime for this iron slag-substituted matrix.

4. CONCLUSIONS

This study successfully established the feasibility of substituting CFA with IS in GMC, addressing critical sustainability and resource availability challenges, particularly in regions lacking CFA reserves. Microstructural analyses confirmed that both precursors provide the essential glass-forming oxides requisite for geopolymerization, albeit through distinct gel formation mechanisms dictated by their compositional variations. While the benchmark CFA mix (yielding 3.241 MPa) relies on abundant silica and alumina to develop robust aluminosilicate networks, the optimized IS-substituted matrix incorporating 30% IS and cured at 60 °C for 24 hours drives binder formation through complex Fe-A-S-H and C-A-S-H gels to achieve a maximum 28-day compressive strength of 1.601 MPa.

This mechanical performance demonstrates clear practical feasibility, as compressive strengths in the 1–2 MPa range align with or exceed the minimum requirements of several international standards for non-load-bearing masonry units, such as partition walls (Raja et al., 2023). Furthermore, literature highlights that IS-based geopolymer concretes often exhibit continued strength gain well beyond 28 days under favorable curing regimes, adding to their long-term structural value. However, it is important to note that while a 1.6 MPa capacity is highly suitable for non-structural applications, it may not suffice for environments requiring higher load resistance or severe exposure conditions without further optimization. Ultimately, IS-based GMC serves as an eco-friendly, locally accessible alternative that effectively advances industrial waste valorization and sustainable construction practices.

5. RECOMMENDATIONS FOR FUTURE WORK

Future research should prioritize the blending of multi-precursors to address the current load-bearing limitations and further advance the deployment of IS-based geopolymers. Additionally, exploring alternative chemical activation parameters, such as adjusting sodium hydroxide molarity or modifying the silicate-to-hydroxide ratio, may unlock further reactivity within the IS matrix. Finally, to fully validate the real-world applicability of these eco-friendly masonry units, comprehensive Life-Cycle Assessments (LCA) and long-term durability evaluations must be conducted.

6. REFERENCES

Arooz, F. R. (2019). *In-situ Mud-Concrete as a material for load-bearing walls and sustainable building practices* [Doctoral dissertation, University of Moratuwa]. University of Moratuwa Institutional Repository. http://dl.lib.uom.lk/handle/123/16439

Arooz, F. R., & Halwatura, R. U. (2018). Case Studies in Construction Materials Mud-concrete block (MCB): mix design & durability characteristics. *Case Studies in Construction Materials*, 8(June 2017), 39–50. https://doi.org/10.1016/j.cscm.2017.12.004

Chen, Y., Fan, Y., Huang, Y., Liao, X., Xu, W., & Zhang, T. (2024). A comprehensive review of toxicity of coal fly ash and its leachate in the ecosystem. *Ecotoxicology and Environmental Safety*, 269, 115905. https://doi.org/10.1016/j.ecoenv.2023.115905

Ferreira, R. L. S., Medeiros, M., Pereira, J. E. S., Henriques, G. F., Tavares, J. C., Marvila, M. T., & de Azevedo, A. R. G. (2023). Effects of Particle Size Distribution of Standard Sands on the Physical-Mechanical Properties of Mortars. *Materials,* 16(2), 844. https://doi.org/10.3390/ma16020844

Gayashani, K. G. C., Piyasena, R. K. N. P., Oshadhi, D. A., Young, S. M., & Halwatura, R. U. (2025). Utilization of textile industry by-products to develop and optimize geopolymerized mud concrete for sustainable construction.In K. G. A. S. Waidyasekara, H. S. Jayasena, P. L. I. Wimalaratne, & G. A. Tennakoon (Eds.), *Proceedings of the 13th World Construction Symposium*. University of Moratuwa. https://doi.org/10.31705/WCS.2025.108

Hao, J., Zhou, Z., Chen, Z., Zhao, Z., & Shen, Y. (2025). Mechanical performance and damage mechanisms of steel slag-cement pasted backfill under high-temperature cured and cyclic static loading for deep-mining applications. *Journal of Materials Research and Technology*, 35, 5698–5716. https://doi.org/10.1016/j.jmrt.2025.02.150

Haustein, E. and Kuryłowicz-Cudowska, A. (2020), "The effect of fly ash microspheres on the pore structure of concrete", *Minerals*, Vol. 10 No. 1, p. 58, doi: 10.3390/min10010058.

Juenger, M. C. G., Winnefeld, F., Provis, J. L., & Ideker, J. H. (2011). Advances in alternative cementitious binders. *Cement and Concrete Research*, 41(12), 1232–1243. https://doi.org/10.1016/j.cemconres.2010.11.012

Pławecka, K., Bazan, P., Lin, W.-T., Korniejenko, K., Sitarz, M., & Nykiel, M. (2022). Development of geopolymers based on fly ashes from different combustion processes. *Polymers*, 14(10), 1954. https://doi.org/10.3390/polym14101954

Lee, N. K., & Lee, H. K. (2015). Reactivity and reaction products of alkali-activated, fly ash/slag paste. *Construction and Building Materials*, 81, 303–312. https://doi.org/10.1016/j.conbuildmat.2015.02.022

Lee, Y. H., Eom, H., Lee, S. M., & Kim, S. S. (2021). Effects of pH and metal composition on selective extraction of calcium from steel slag for Ca(OH)2 production. *RSC Advances*, 11(14), 8306–8313. https://doi.org/10.1039/d0ra08497b

Ma, J., Wang, D., Zhao, S., Duan, P., & Yang, S. (2021). Influence of particle morphology of ground fly ash on the fluidity and strength of cement paste. *Materials*, 14(2), 283. https://doi.org/10.3390/ma14020283

Mohan K, S. M., Kinuthia, J. M., Oti, J., & Adeleke, B. (2025). Geopolymer chemistry and composition: A comprehensive review of synthesis, reaction mechanisms, and material properties—Oriented with sustainable construction. *Materials, 18*(15), 5432.

Nath, S. K., & Kumar, S. (2013). Influence of iron making slags on strength and microstructure of fly ash geopolymer. *Construction and Building Materials,* 38, 924–930. https://doi.org/10.1016/j.conbuildmat.2012.09.070

Nikolov, A. (2020). Alkali-activated geopolymers based on iron-rich slag from copper industry. *IOP Conference Series: Materials Science and Engineering*, 951, 012006. https://doi.org/10.1088/1757-899x/951/1/012006

Raja, V. K. B., Selvarani, V., Kannan, S., Sujan, S., Sahas, S., Padmapriya, R., Kumar, V. G., & Baalamurugan, J. (2023). Geopolymer based foams from steel slag – A green technology. *Materials Today: Proceedings*. https://doi.org/10.1016/j.matpr.2023.07.156

Shi, X., Zhang, C., Liang, Y., Luo, J., Wang, X., Feng, Y., Li, Y., Wang, Q., & Abomohra, A. (2021). Life cycle assessment and impact correlation analysis of fly ash geopolymer concrete. *Materials, 14*(23), 7222

Singh, N. B., & Middendorf, B. (2020). Geopolymers as an alternative to Portland cement: An overview. *Construction and Building Materials*, 237, 117455. https://doi.org/10.1016/j.conbuildmat.2019.117455

Strzałkowska, E. (2020). Morphology and chemical composition of mineral matter present in fly ashes of bituminous coal and lignite. *International Journal of Environmental Science and Technology*, 18(9), 2533–2544. https://doi.org/10.1007/s13762-020-03016-0

Udawattha, C., & Halwatura, R. (2018). Case Studies in Construction Materials Geopolymerized self-compacting mud concrete masonry units. *Case Studies in Construction Materials*, 9, e00177. https://doi.org/10.1016/j.cscm.2018.e00177

United Nations Environment Programme. (2023). *Building materials and the climate: Constructing a new future*. https://www.unep.org/resources/report/building-materials-and-climate-constructing-new-future

Verma, M., & Nigam, M. (2023). Investigation on the effect of curing time on the mechanical properties of geopolymer concrete. *AIP Conference Proceedings*. https://doi.org/10.1063/5.0154116

Wang, C., Wu, Y., Xie, L., Yang, Z., Tian, J., Yu, F., Ren, J., & Li, S. (2025). Estimating soil-water characteristic curve from the particle size distribution with a novel granular packing model. *Water Resources Research*, 61(2). https://doi.org/10.1029/2024wr037262

Wang, M., Xu, J., Zhang, X., Tan, L., & Mei, Y. (2024). Mechanical performance optimization and microstructural mechanism study of alkali-activated steel slag–slag cementitious materials. *Buildings*, 14(5), 1204. https://doi.org/10.3390/buildings14051204

Wijepala, W. M. T. B., Young, S. M., & Ishiga, H. (2022). Ancient metalworking at Yodhawewa site, Sri Lanka: Tracing the archaeological and geochemical relationship by analyzing soil and slags. *Archaeological and Anthropological Sciences*, 15(1). https://doi.org/10.1007/s12520-022-01704-1

Zhang, S., Li, Z., Ghiassi, B., Yin, S., & Ye, G. (2021). Fracture properties and microstructure formation of hardened alkali-activated slag/fly ash pastes. Cement and Concrete Research, 144, 106447. https://doi.org/10.1016/j.cemconres.2021.106447